

## MIT Open Access Articles

*Transplanting assembly of carbon-nanotube-tipped atomic force microscope probes*

The MIT Faculty has made this article openly available. **Please share** how this access benefits you. Your story matters.

**Citation:** Kim, Soohyung, Hyung Woo Lee, and Sang-Gook Kim. "Transplanting Assembly of Carbon-nanotube-tipped Atomic Force Microscope Probes." *Applied Physics Letters* 94.19 (2009): 193102. Web.

**As Published:** <http://dx.doi.org/10.1063/1.3136762>

**Publisher:** American Institute of Physics

**Persistent URL:** <http://hdl.handle.net/1721.1/75217>

**Version:** Final published version: final published article, as it appeared in a journal, conference proceedings, or other formally published context

**Terms of Use:** Article is made available in accordance with the publisher's policy and may be subject to US copyright law. Please refer to the publisher's site for terms of use.



## Transplanting assembly of carbon-nanotube-tipped atomic force microscope probes

Soohyung Kim, Hyung Woo Lee, and Sang-Gook Kim<sup>a)</sup>

Department of Mechanical Engineering, Massachusetts Institute of Technology, 77 Massachusetts Ave., Cambridge, Massachusetts 02139, USA

(Received 27 December 2008; accepted 22 April 2009; published online 13 May 2009)

Carbon-nanotube (CNT)-tipped atomic force microscope (AFM) probes were assembled in a deterministic and reproducible manner by transplanting a CNT bearing polymeric carrier to a microelectromechanical systems cantilever. Single-strand CNTs were grown vertically at predefined locations where each CNT was encapsulated into a cylindrical polymer carrier block. Double-layer carriers were used for controlling the release of blocks and the exposed length of CNT tips after the assembly. Much reduced complexity in assembly was achieved by transplanting individual CNTs to AFM probes, which could scan nanotrenches and biostructures with little probe artifacts. © 2009 American Institute of Physics. [DOI: 10.1063/1.3136762]

Carbon nanotubes (CNTs) have attracted much attention due to their excellent mechanical, electrical, chemical, and thermal properties. Various potential applications have been suggested and demonstrated,<sup>1</sup> which would require the assembly of CNTs with a control of their location, orientation, and geometrical configurations. Promising efforts have been reported to locate and assemble nanostructures such as CNTs with the Langmuir–Blodgett technique, fluid flow and capillary forces, external forces, and templates, among many.<sup>2–4</sup> An assembly of some functional nanodevices, however, requires locating an individual nanostructure at a deterministic position of micro- or mesoscale structures, which is still a very complex task. A CNT-tipped probe for an atomic force microscope (AFM) is a typical application, which requires an assembly of a single-strand CNT at the tip of an AFM cantilever. The degree of complexity increases rapidly as the assembly system's scale order grows, which can be defined as the logarithmic ratio of the size of the target assembly system to the smallest characteristic length of its nanoscale component. In this letter, we report that transplanting assembly of individual CNTs can reduce the complexity of assembly by encapsulating individual CNTs into microcarrier blocks and demonstrate that this method can be used to make CNT-tipped AFM probes efficiently.

The nanometer-scale diameter, high-aspect-ratio cylindrical geometry, easy buckling under excessive load, and superior wear resistance of CNTs make the CNT-tipped AFM probe a tool for high-resolution imaging and scanning of nano- and biostructures.<sup>5,6</sup> However, the volume manufacture of these has been a challenging task due to the complexity of handling and locating only one CNT tip at the apex of an AFM cantilever. Previous approaches to the fabrication of CNT-tipped AFM probes include attaching a CNT at the apex of an AFM probe manually,<sup>5</sup> with a guidance of the external magnetic<sup>7</sup> and electric fields,<sup>8</sup> pick-and-place using an AFM device,<sup>9</sup> or growing CNTs at embedded catalytic metal seeds at the apex of AFM probes.<sup>10</sup> All approaches showed good functionality of CNT-tipped AFM probes but required time-consuming effort such as removing redundant

CNT tips and shortening, aligning, or welding CNT tips.

Transplanting a bundle of CNTs was demonstrated by one of the authors previously.<sup>11</sup> By decoupling growing from assembling CNTs, transplanting assembly showed a potential that a high rate production of CNT-based devices could be achieved. But the previous method could not handle or assemble individual CNTs. We report a method for the deterministic assembly of individual CNTs, which consists of growing an array of vertically aligned single-strand CNTs, encapsulating each CNT into a microscale polymer carrier block, which can be handled and manipulated with existing microscale tools, and transplanting the CNT-bearing polymer blocks to target locations followed by the exposure of buried CNTs. Figure 1 summarizes the transplanting assembly process we designed to make a CNT-tipped AFM probe. The geometry and the orientation of individual CNTs are frozen into photosensitive polymer layers spin casted over an array of single-strand CNTs vertically grown at the predefined locations on a silicon substrate. Then the photosensitive polymer layers are lithographically patterned to form cylindrical blocks over the individual CNTs, which is similar to the cookie-cutting process. An intentional undercut of the bottom layer holds the carrier blocks until the release from the substrate and controls the exposed length of the CNT tips after assembly.

The first step in transplanting assembly is the vertical growth of CNTs, which requires seeding the nickel (Ni) catalytic nanodots at predefined locations on the Si substrate. A  $21 \times 21$  array of Ni catalytic dots (100–200 nm in diameter and 30 nm in thickness) was defined using electron beam lithography (Raith 150 at MIT's Scanning Electron Beam

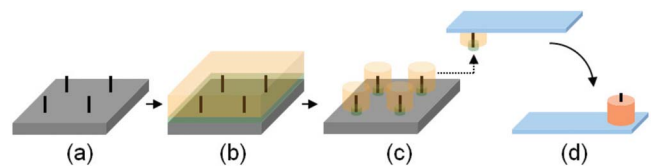


FIG. 1. (Color online) Transplanting assembly process steps for CNT-tipped AFM probes. (a) Vertical CNT growth, (b) encapsulation, (c) cookie cutting (forming individual polymer block containing a single CNT tip at the bottom with intentional undercut), and (d) CNT tip release.

<sup>a)</sup>Author to whom correspondence should be addressed. Electronic mail: sangkim@mit.edu.

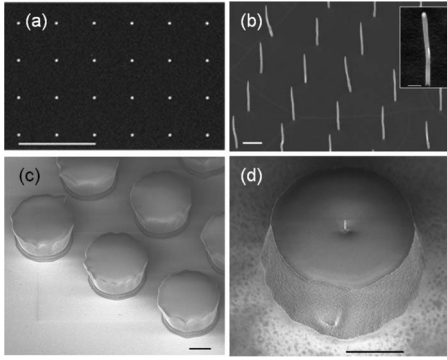


FIG. 2. The growth and encapsulation of an array of vertically aligned individual CNTs. (a) An array of 30 nm thick Ni dots formed by electron beam lithography (scale bar: 10  $\mu\text{m}$ ). (b) An array of vertically grown CNT strands (scale bar: 2  $\mu\text{m}$ ). The inset shows a freestanding CNT, 150 nm in diameter and 5  $\mu\text{m}$  in length (scale bar: 500 nm). (c) An array of SU8 blocks encapsulating CNTs (scale bar: 10  $\mu\text{m}$ ). (d) An SU8 block shows a single CNT after release (scale bar: 10  $\mu\text{m}$ ).

Lithography Facility) followed by metal deposition and lift-off process. An array of vertically aligned CNTs was grown using a home-built plasma enhanced chemical vapor deposition machine.<sup>12</sup> Each CNT strand was then embedded into a micropolymer block, which serves as a CNT carrier. We used a double polymeric layer encapsulation process with SU8 (top: MicroChem) and polymethylglutarimide (PMGI) (bottom: MicroChem): the top SU8 (15  $\mu\text{m}$  in thickness and 20  $\mu\text{m}$  in diameter) forms the body of the carrier, while the bottom PMGI layer (1.5  $\mu\text{m}$  in thickness) holds the body until the release of the carrier from the substrate and then is removed to expose the CNT tip. Figure 2 shows Ni catalytic dots defined using electron beam lithography [Fig. 2(a)], an array of vertically grown CNT strands [Fig. 2(b)], an array of SU8 pillars encapsulating individual CNTs [Fig. 2(c)], and an inverted SU8 block bearing a single CNT tip [Fig. 2(d)]. The orientation of the embedded CNT is near parallel to the axis of the SU8 block. The diameter of CNTs matches the size of Ni dots, and the length is 5–10  $\mu\text{m}$  with a uniform cylindrical shape. The thickness of the bottom PMGI layer was chosen to be 1.5  $\mu\text{m}$  so that a target aspect ratio of the CNT tip is about 10, which would give about 0.1 nm thermal fluctuation at the end of the tip at room temperature (300 K). The 20  $\mu\text{m}$  diameter of SU8 blocks was the result of process constraints in our facility, which can be further reduced to achieve the higher resonance frequency and the higher aspect ratio of the probes.

We investigated the physicochemical interaction of individual CNTs to see whether the pristine properties of CNTs can be preserved during the transplanting process, and the vertical orientation of grown CNTs can be maintained under the fluidic shearing during the spin coating of polymers. High-resolution transmission electron microscopy pictures show the same graphene layers with 0.34 nm spacing before and after the encapsulation process, indicating that pristine graphene structures are intact throughout the encapsulation processes. In order to predict the flow-induced deflection during the spin coating of polymers, the polymer spin-coating process is modeled as a one-dimensional (radial direction) laminar flow by the centrifugal force and shearing force, as shown in

$$U(r, z) = \frac{\omega^2 R z}{\nu} \left( t - \frac{z}{2} \right), \quad (1)$$

where  $\omega$  is the rotational speed,  $R$  is the distance from the center of rotation,  $z$  is the height from the substrate,  $\nu$  is the viscosity of a polymer, and  $t$  is the thickness of the polymer layer. The corresponding Reynolds number is about  $5 \times 10^{-4}$  at the maximum velocity, indicating a laminar flow. The array of vertically aligned CNTs packed within a  $1 \times 1 \text{ mm}^2$  area is located near the central position of the spin axis, and each CNT is modeled as a rod rigidly clamped to the substrate with the assumption of no-slip condition on the substrate. Drag coefficients are calculated using the radial velocity distributions along the CNT, and force distributions are obtained from the drag coefficients in

$$C_D = \left( \frac{8\pi}{\text{Re} \ln(7.4/\text{Re})} \right) \left( \frac{3 + 2\phi^{5/3}}{3 - 4.5\phi^{1/3} + 4.5\phi^{5/3} - 3\phi^2} \right), \quad (2)$$

$$F_D = \frac{1}{2} C_D \rho U^2 A, \quad (3)$$

where  $\phi$  is the areal fill factor of CNT strands in each cell. The final deflection at the end of a CNT tip is calculated using a linear beam bending model under distributed loads, which predicts less than  $1^\circ$  deflection from the vertical axis. This small deflection with respect to the dimension of CNT tips (150 nm in diameter and 1.5  $\mu\text{m}$  in length) is negligible and matches with the observation at the transplanted CNT tips [Fig. 2(d)].

After encapsulation, a polymer block where a single-strand CNT is embedded is transplanted manually to the end of a silicon cantilever using the micromotion probe stage under an optical microscope. A tipless AFM cantilever (NCS12, MicroMasch), which already picked a drop of liquid adhesive (LOCTITE® 408), approaches a target pellet. When the adhesive is dried, the pellet attached to the end of the AFM cantilever is released by gently shearing the pellet. After assembly, we etch any remaining PMGI bottom layer and expose a CNT tip of about 1.5  $\mu\text{m}$ , which corresponds to the bottom (PMGI) layer thickness. Various CNT-tipped AFM probes for different scanning operation modes were fabricated by assembling a CNT embedded SU8 pellet on various AFM cantilevers. Figure 3 shows AFM probes with a transplanted single-strand CNT. The fact that even a manual assembly of CNT is feasible shows that the complexity of assembly has been reduced by encapsulating CNTs into microcarrier blocks. CNT-tipped AFM probes for different modes of scanning could be produced by transplanting assembly of individual CNTs on various cantilevers (Si- and Au-coated  $\text{Si}_3\text{N}_4$  cantilevers), which demonstrates the flexibility of transplanting assembly as a viable manufacturing process for CNT-tipped probes.

The performance of transplanting-assembled AFM probes was tested by mounting them on a commercial AFM (DI 3100, Veeco Instruments Inc.) and scanning over an AFM calibration grating (TGZ02, MikroMasch). The Si grating consists of 106 nm deep vertical trenches with a period of 3  $\mu\text{m}$ . We used the contact mode scanning with a scanning range of  $10 \times 10 \mu\text{m}^2$  and a scanning speed of 10  $\mu\text{m}/\text{s}$ . The transplanting-assembled CNT AFM probes scanned the vertical walls of trenches with sidewall angles larger than  $85^\circ$ , which shows much less probe artifact than

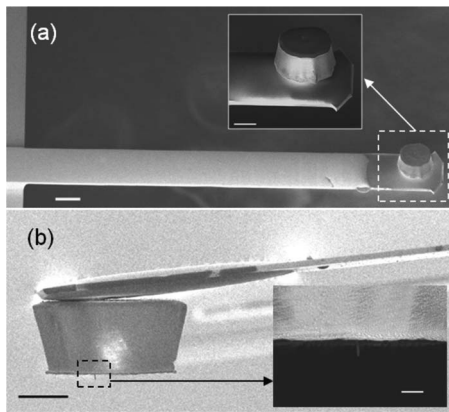


FIG. 3. CNT-tipped AFM probes made by transplanting assembly. (a) A contact mode probe on a Si cantilever with a spring constant of 0.3 N/m (scale bar: 20  $\mu\text{m}$ ). The inset shows the enlarged view of the CNT tip (scale bar: 10  $\mu\text{m}$ ). (b) The side view of a tapping mode CNT-tipped AFM probe with a tuned resonance frequency of 60 kHz (scale bar: 10  $\mu\text{m}$ ). The inset shows the vertical CNT tip (scale bar: 2  $\mu\text{m}$ ).

that with the standard Si probe (Fig. 4). We also scanned soft protein structures such as actin filament (F-actin) samples, as shown in Fig. 5. F-actin was prepared in a buffer solution and stored at 4 °C before scanning. 10 ml of the solution was dropped on a glass slide, and AFM scanning was performed after the solution had dried.

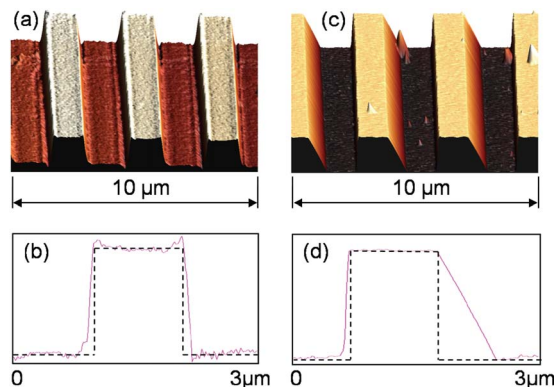


FIG. 4. (Color online) Comparison of AFM scanning results on an AFM calibration grid. (a) A scanning result with a CNT-tipped AFM probe (contact mode). (b) The sectional profile of (a) where the dotted line represents the ideal shape of 106 nm deep trenches and the solid line denotes the scanning results. (c) Scanning result with a standard Si AFM probe (tapping mode). (d) The sectional profile of (c).

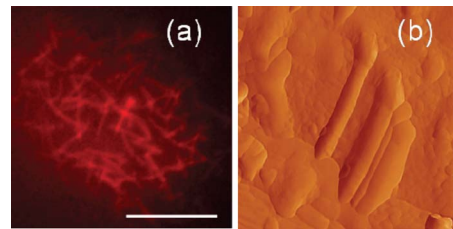


FIG. 5. (Color online) The scanning of a biological sample (64  $\mu\text{l}$ /2.3  $\mu\text{M}$  of F-actin) with a CNT-tipped AFM probe. (a) Fluorescent microscopy shows bundles of F-actins in the buffer solution (scale bar: 10  $\mu\text{m}$ ). (b) AFM scanning image of F-actins (scanning range:  $3 \times 3 \mu\text{m}^2$ ).

We demonstrated that transplanting assembly could assemble individual CNTs into microscale cantilevers at much reduced complexity. This could be achieved by shifting the scale order of assembly from “nano/micro” to “micro/micro,” thus reducing the complexity of the assembly. Transplanting assembly enables even manual assembly of a CNT-tipped AFM probe to be done in minutes excluding the adhesive curing time. We believe that this assembly method can be scaled up and automated to make a massive parallel assembly of nanostructures for high throughput applications.

The authors thank Intelligent Microsystems Center in Korea, DARPA Grant No. HR0011-06-1-0045, and Hewlett Packard for a partial funding of this research. The first and the second author contributed equally to this work.

- <sup>1</sup>R. H. Baughman, A. A. Zakhidov, and W. A. de Heer, *Science* **297**, 787 (2002).
- <sup>2</sup>Y. Huang, X. Duan, Q. Wei, and C. M. Lieber, *Science* **291**, 630 (2001).
- <sup>3</sup>Y. Cui, M. T. Bjork, J. A. Liddle, C. Sonnichsen, B. Boussert, and A. P. Alivisatos, *Nano Lett.* **4**, 1093 (2004).
- <sup>4</sup>P. A. Smith, C. D. Nordquist, T. N. Jackson, T. S. Mayer, B. R. Martin, J. Mbindyo, and T. E. Mallouk, *Appl. Phys. Lett.* **77**, 1399 (2000).
- <sup>5</sup>H. Dai, J. H. Hafner, A. G. Rinzler, D. T. Colbert, and R. E. Smalley, *Nature (London)* **384**, 147 (1996).
- <sup>6</sup>T. Larsen, K. Moloni, F. Flack, M. A. Eriksson, M. G. Lagally, and C. T. Black, *Appl. Phys. Lett.* **80**, 1996 (2002).
- <sup>7</sup>A. Hall, W. G. Matthews, R. Superfine, M. R. Falvo, and S. Washburn, *Appl. Phys. Lett.* **82**, 2506 (2003).
- <sup>8</sup>J. Tang, G. Yang, Q. Zhang, A. Parhat, B. Maynor, J. Liu, L. Qin, and O. Zhou, *Nano Lett.* **5**, 11 (2005).
- <sup>9</sup>J. H. Hafner, C. Cheung, T. H. Oosterkamp, and C. M. Lieber, *J. Phys. Chem. B* **105**, 743 (2001).
- <sup>10</sup>Q. Ye, A. M. Cassell, H. Liu, K. Chao, J. Han, and M. Meyyappan, *Nano Lett.* **4**, 1301 (2004).
- <sup>11</sup>T. El-Aguizy, J.-h. Jeong, Y. B. Jeon, W. Z. Li, Z. F. Ren, and S. G. Kim, *Appl. Phys. Lett.* **85**, 5995 (2004).
- <sup>12</sup>Z. F. Ren, Z. P. Huang, J. W. Xu, J. H. Wang, P. M. Bush, P. Siegal, and P. N. Provencio, *Science* **282**, 1105 (1998).